Available online at www.sciencedirect.com

ScienceDirect

Journal of Sound and Vibration 304 (2007) 201–212

JOURNAL OF SOUND AND VIBRATION

www.elsevier.com/locate/jsvi

# Parametrically excited vibrations of an oscillator with strong cubic negative nonlinearity

Livija Cveticanin*, Ivana Kovacic

*Faculty of Technical Sciences, 21000 Novi Sad, Trg D. Obradovica 6, Serbia*

Received 16 August 2006; received in revised form 15 February 2007; accepted 19 February 2007

**Abstract**

In this paper the parametrically excited vibrations of an oscillator with strong cubic negative nonlinearity are analyzed. The two-dimensional Lindstedt–Poincare perturbation technique applied for finding an approximate solution of linear parametrically excited systems is extended for analyzing a strong nonlinear oscillator. Based on the solution of a nonlinear differential equation with constant coefficients, an approximative solution is introduced. The transition curves and transient surfaces along which periodic solutions exist are obtained. Their strong dependence on the initial conditions is evident. To prove the analytical solution, the numerical experiment is done. For certain values initial conditions and parameter values, the time history diagrams for the oscillator are plotted.


## 1. Introduction

Parametrically excited systems are widely spread in many branches of physics and engineering. In mechanical and elastic systems, parametrically excited vibrations occur due to time varying loads, especially periodic ones. These vibrations appear in columns made of nonlinear elastic material [1], beams with a harmonically variable length [2], beams with harmonic motion of their support [3], floating offshore structures [4], parametrically excited pendulums [5], cables being towed by a submarine [6,7], etc. Parametric excitations occur in electrostatically driven microelectro-mechanical oscillators [8], which is produced by fluctuating voltages applied across comb drives. In practical engineering situations the properties of parametric oscillations are widely used, for example, in the radio, the computer and laser engineering, in vibromachines with special design [9], Paul trap mass spectrometers [10] and a simulator for proving the equivalence of inertia and passive gravitational mass [11]. Parametric resonance has been well established in many areas of science, including the stability of ships, the forced motion of a swing and Faraday surface wave patterns on water. The highly sensitive mass sensor is studied as an in-plane parametrically resonant oscillator [12].

The simplest mathematical model of the system with a parametric periodic load is usually a linear Mathieu differential equation. Due to the nonlinear properties of a real system, nonlinear terms are added to the equation [13]. Usually, they are of a cubic type and the differential equation is transformed to the

*Corresponding author.
*E-mail address:* cveticanin@uns.ns.ac.yu (L. Cveticanin).

0022-460X/$ - see front matter 
doi:10.1016/j.jsv.2007.02.028

Mathieu–Duffing equation [14]. To determine the combined effect of nonlinearities and parametric excitations, numerous analytical techniques have been developed. Two classes of these techniques are dominant. One class is based on the integral of energy and numerical integration [15]. The method is suitable for obtaining the boundaries between bounded and unbounded solutions of the equation. The advantage of the method is that it gives accurate stability charts, but the procedure is time consuming. If the energy integral represents the Lyapunov function, then Lyapunov stability theory is also applicable. With this approach, it is possible to determine qualitatively the general stability of the system, but one cannot determine qualitatively the system response.

The second technique, which is much more developed, consists of the perturbation methods that are based on the assumption that the variable-coefficient terms are small in some sense. The most widely applied is the method of multiple scales [16]. The method is used to obtain solutions that are valid in neighborhoods close to the transient curves. The method of multiple scales is extended for solving the stochastic Mathieu–Duffing equation, too. The almost sure-stability criterion and instability criterion are determined [17].

Ng and Rand [6,7] investigated the Mathieu–Duffing equation using another perturbation method. They showed that the averaging method is suitable for solving the deterministic Mathieu oscillator.

The method of strained parameters [16] is also an asymptotic analytical method, which is well suited for the determination of the transient curves between stable and unstable solutions. This method yields a solution which is valid right on the transient curve and does not yield a solution that is valid in the neighborhood close to the transient curve. Following this method and based on Floquet theory, if one assumes that the solutions have periods of $\pi$ and $2\pi$, then, the values of the parameters for which this assumption is true can be determined [16].

All the previous techniques have been applied to solve differential equations with a small parametric excitation and small nonlinearity. Zounes and Rand [18] considered the Mathieu–Duffing oscillator, assuming that the parametric perturbation is small but the coefficient of the nonlinear term is positive and not necessary small.

In this paper the Mathieu–Duffing equation with a small parametric excitation and strong negative nonlinearity is investigated. The mathematical model corresponds to the parametrically excited oscillator with a softening spring. The aim of the paper is to obtain the transient values of the parameters of the system which lead the periodic solutions. The two-dimensional Lindstedt–Poincare perturbation technique is adopted for solving the differential equation

$$\ddot{x} + (\delta + 2\varepsilon\cos 2t)x - \varphi x^3 = 0, \tag{1}$$

with the initial conditions

$$x(0) = X_0, \quad \dot{x}(0) = \dot{X}_0, \tag{2}$$

where $\varphi$ is the parameter of nonlinearity and $\varepsilon \ll 1$ is a small parameter. In contrast to the previous perturbation treatments, the unperturbed system is nonlinear and the use of the elliptic functions, instead of the trigonometric functions, which have been applied for the linear systems, is introduced. The regions of stability and instability, i.e., the bounded and unbounded solutions of the Mathieu–Duffing equation are discussed.

## 2. Solution procedure

The perturbation expansions of the function $x$ and parameter $\delta$ are introduced

$$x(t,\varepsilon) = x_0(t) + \varepsilon x_1(t) + \cdots, \tag{3}$$

$$\delta = \delta_0 + \varepsilon\delta_1 + \cdots. \tag{4}$$

Substituting Eqs. (3) and (4) into Eqs. (1) and (2) and equating coefficients of similar powers of $\varepsilon$, we obtain

$$\ddot{x}_0 + \delta_0 x_0 - \varphi x_0^3 = 0,$$

$$\ddot{x}_1 + \delta_0 x_1 - 3\varphi x_0^2 x_1 = -\delta_1 x_0 - 2x_0\cos 2t, \tag{5}$$

and

$$x_0(0) = X_0, \quad \dot{x}(0) = \dot{X}_0,$$
$$x_1(0) = 0, \quad \dot{x}_1(0) = 0, \tag{6}$$

Eq. $(5)_1$ is a differential equation with strong cubic nonlinearity, which has a periodic solution of the form

$$x_0 = A_0 \,\mathrm{sn}(\omega_0 t + \alpha_0, k_0), \tag{7}$$

where sn is the elliptic function [19] with the frequency $\omega_0$ and the modulus $k_0$ given respectively by

$$\omega_0^2 = \delta_0 - \frac{\varphi A_0^2}{2}, \quad k_0^2 = \frac{\varphi A_0^2}{2(\delta_0 - (\varphi A_0^2/2))}, \tag{8}$$

and $A_0$ and $\alpha_0$ are arbitrary constants. The motion is periodic for $A_0 < \sqrt{2\delta_0/\varphi}$.

The elliptic function sn has the period $4nK(k)$, where $K(k)$ is the complete elliptic integral of the first kind [19] and $n = 0, 1, 2, \ldots$ .

(1) For $n = 0$ we obtain $\omega_0 = 0$. If the initial velocity is zero ($\dot{X}_0 = 0$) Eqs. (7) and (8) results in

$$x_0 = X_0 = \mathrm{const.} \tag{9}$$

and

$$\delta_0 = \varphi X_0^2. \tag{10}$$

Because $x_0$ is constant, Eq. (5) becomes an ordinary non-homogenous differential equations, of the form

$$\ddot{x}_1 - 2\varphi X_0^2 x_1 = -\delta_1 X_0 - 2X_0 \cos 2t. \tag{11}$$

Solving Eq. (11) with the initial conditions given in Eq. $(6)_2$, we obtain

$$x_1 = \frac{\delta_1}{2\varphi X_0} - \left(\frac{\delta_1}{2\varphi X_0} + \frac{X_0}{2 + \varphi X_0^2}\right) \mathrm{ch}(X_0 t\sqrt{2\varphi}) + \frac{X_0}{2 + \varphi X_0^2} \cos 2t. \tag{12}$$

The periodic solution

$$x_1 = -\frac{X_0}{2 + \varphi X_0^2}(1 - \cos 2t), \tag{13}$$

exists for

$$\delta_1 = -\frac{2\varphi X_0^2}{2 + \varphi X_0^2}. \tag{14}$$

Using Eqs. (4), (10) and (14), the transient curve in the first approximation is given by

$$\delta = \varphi X_0^2 \left(1 - \frac{2\varepsilon}{2 + \varphi X_0^2}\right) \tag{15}$$

and along this curve the solution is

$$x = X_0 - \frac{\varepsilon X_0}{2 + \varphi X_0^2} + \frac{\varepsilon X_0}{2 + \varphi X_0^2} \cos 2t. \tag{16}$$

To confirm the correctness of the analytical procedure, the analytical result (16) is compared with the numerical solution obtained by solving Eq. (1) with Eq. (15) for the initial conditions $x_0(0) = X_0 = 0.1$, $\dot{x}(0) = 0$. In Fig. 1 the time histories $x(t)$ are plotted for $X_0 = 0.1$, $\varphi = 2$ and various values of the small parameter: $\varepsilon = 0.01$ (Fig. 1a) and $\varepsilon = 0.1$ (Fig. 1b). It is evident that during the initial time period the difference between the analytical and numerical solutions is negligible.

(2) For the period $4K(k)$ the frequency is $\omega_0 = 1$ and

$$\delta_0 = 1 + \frac{\varphi A_0^2}{2}, \quad k_0^2 = \frac{\varphi A_0^2}{2}, \tag{17}$$

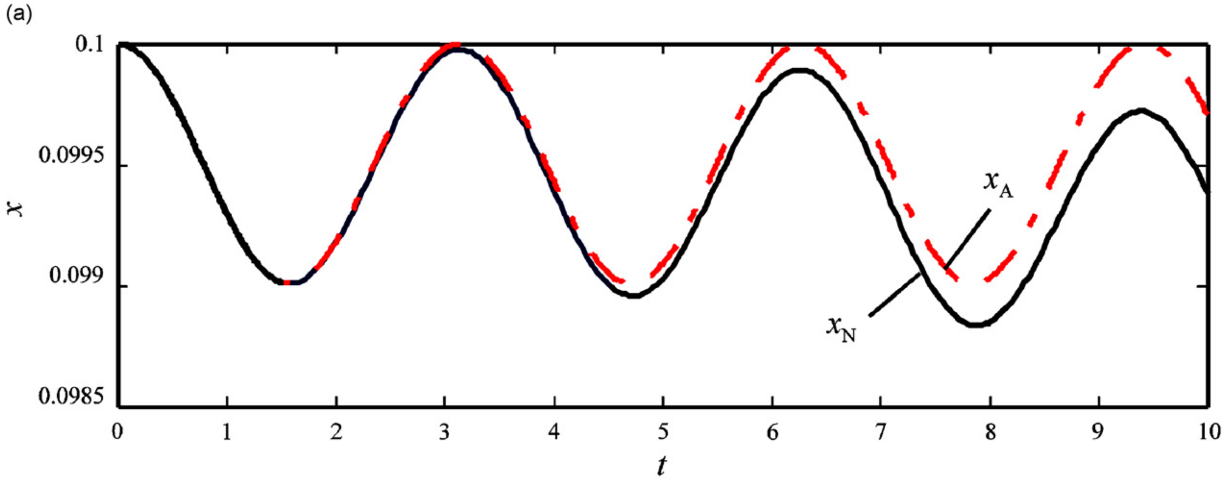


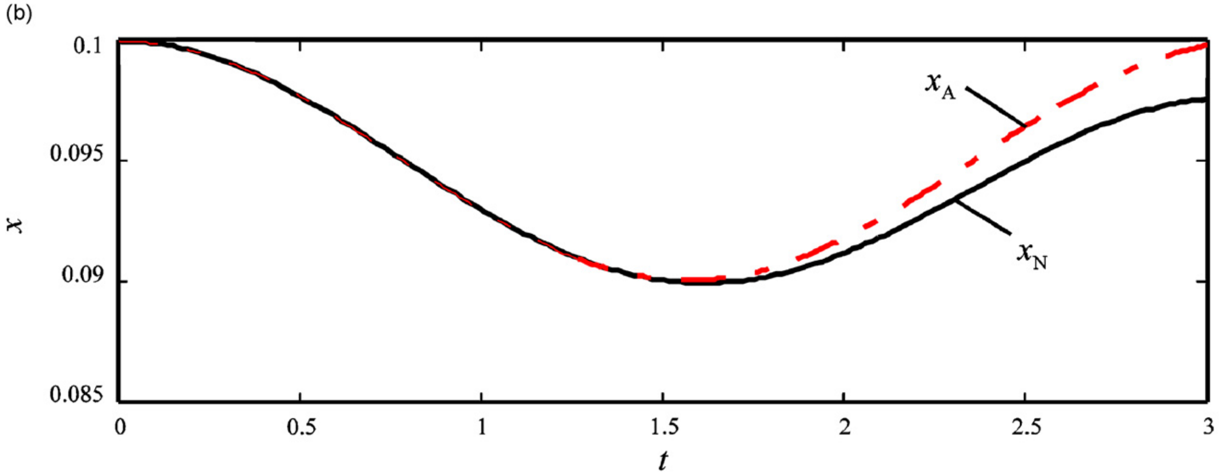


Fig. 1. The history diagrams $x$-$t$ obtained analytically ($x_A$) and numerically ($x_N$) for the following parameter values $\varphi = 2$, $x(0) = 0.1$, $\dot{x}(0) = 0$: (a) $\varepsilon = 0.01$, (b) $\varepsilon = 0.1$.

where the arbitrary amplitude is (see Eqs. $(6)_1$ and (7))

$$A_0 = \sqrt{X_0^2 + \frac{\dot{X}_0^2}{1 - (\varphi/2)X_0^2}}. \tag{18}$$

The initial phase $\alpha_0$ satisfies the relation

$$\mathrm{sn}\left(\alpha_0, \frac{\varphi A_0^2}{2}\right) = \frac{X_0}{A_0}. \tag{19}$$

Using the transformation given in Ref. [20], relation (7) is transformed into

$$x_0 = A_0 \frac{\mathrm{sn}_0 C_0 D_0 - \mathrm{cn}_0 \mathrm{dn}_0 S_0}{1 - k_0^2 \mathrm{sn}_0^2 S_0^2}, \tag{20}$$

where $\mathrm{cn}_0 \equiv \mathrm{cn}(t, k_0)$, $\mathrm{sn}_0 \equiv \mathrm{sn}(t, k_0)$, $\mathrm{dn}_0 \equiv \mathrm{dn}(t, k_0)$, $S_0 = \mathrm{sn}(\alpha_0, k_0)$, $C_0 = \mathrm{cn}(\alpha_0, k_0)$, $D_0 = \mathrm{dn}(\alpha_0, k_0)$.

Substituting Eq. (20) into Eq. $(5)_2$, yields

$$\ddot{x}_1+\left(1+\frac{\varphi A_0^2}{2}\right)x_1-3\varphi A_0^2\frac{(\mathrm{sn}_0C_0D_0-\mathrm{cn}_0\mathrm{dn}_0S_0)^2}{(1-k_0^2\mathrm{sn}_0^2S_0^2)^2}x_1$$
$$=-\delta_1A_0\frac{\mathrm{sn}_0C_0D_0-\mathrm{cn}_0\mathrm{dn}_0S_0}{1-k_0^2\mathrm{sn}_0^2S_0^2}-2A_0\frac{\mathrm{sn}_0C_0D_0-\mathrm{cn}_0\mathrm{dn}_0S_0}{1-k_0^2\mathrm{sn}_0^2S_0^2}\cos 2t. \tag{21}$$

This equation is a linear parametrically excited differential equation. For the case when $k_0^2\ll 1$, i.e., $\varphi A_0^2/2\ll 1$, the elliptic functions are transformed to the harmonic functions

$$\mathrm{sn}_0\approx\sin t-\frac{k^2}{4}\cos t(t-\sin t\cos t),\quad \mathrm{cn}_0\approx\cos t-\frac{k_0^2}{4}\cos t(t-\sin t\cos t),$$
$$\mathrm{dn}_0\approx 1-\frac{k^2}{2}\sin^2 t. \tag{22}$$

The simplification of expression (20) and the differential equation (21) with Eq. (22) gives

$$x_0=A_0(C_0D_0\sin\sqrt{\Delta}t-S_0\cos\sqrt{\Delta}t)$$

and

$$\ddot{x}_1+\Delta x_1-\varepsilon_1\frac{S_0^2-C_0^2D_0^2}{2}x_1\cos 2t+\varepsilon_1S_0C_0D_0x_1\sin 2t$$
$$=-\delta_1A_0(C_0D_0\sin t-S_0\cos t)-2A_0(C_0D_0\sin t-S_0\cos t)\cos 2t, \tag{23}$$

where $\varepsilon_1$ is a new small parameter

$$\varepsilon_1=3\varphi A_0^2\ll 1, \tag{24}$$

while

$$\Delta=1+\frac{\varepsilon_1}{6}(1-3S_0^2-3C_0^2D_0^2). \tag{25}$$

At this point, the two-dimensional Lindstedt–Poincare expansion is introduced once more. The series expansion with the small parameter $\varepsilon_1$:

$$\delta_1=\delta_{10}+\varepsilon_1\delta_{11}+\cdots,\quad x_1=x_{10}+\varepsilon_1x_{11}+\cdots, \tag{26}$$

is substituted into Eq. (23). After separating the terms with the same order of the small parameter $\varepsilon_1$, the following equations are obtained:

$$\varepsilon_1^0:\quad \ddot{x}_{10}+\Delta x_{10}=-\delta_{10}A_0(C_0D_0\sin\sqrt{\Delta}t-S_0\cos\sqrt{\Delta}t)$$
$$-2A_0(C_0D_0\sin\sqrt{\Delta}t-S_0\cos\sqrt{\Delta}t)\cos 2\sqrt{\Delta}t, \tag{27}$$

$$\varepsilon_1^1:\quad \ddot{x}_{11}+\Delta x_{11}=-\delta_{11}A_0(C_0D_0\sin\sqrt{\Delta}t-S_0\cos\sqrt{\Delta}t)$$
$$+\frac{S_0^2-C_0^2D_0^2}{2}x_{10}\cos 2\sqrt{\Delta}t-S_0C_0D_0x_{10}\sin 2\sqrt{\Delta}t, \tag{28}$$

where

$$\sqrt{\Delta}\approx 1+\frac{\varepsilon_1}{12}(1-3S_0^2-3C_0^2D_0^2). \tag{29}$$

To ensure that $x_{10}$ is periodic, the terms with $\sin\sqrt{\Delta}t$ and $\cos\sqrt{\Delta}t$ in Eq. (27) which lead to secular terms must vanish. This is attainable either for

$$\delta_{10}=-1\quad\text{and}\quad A_0=X_0,\quad C_0=0, \tag{30}$$

or

$$\delta_{10} = 1 \quad \text{and} \quad A_0 = \dot{X}_0, \quad S_0 = 0. \tag{31}$$

If $\delta_{10} = -1$ and the amplitude and phase angle satisfy the relations $A_0 C_0 D_0 = 0$, $A_0 S_0 = X_0$, we obtain the solution of Eq. (27) with the secular terms eliminated

$$x_{10} = \frac{X_0}{8\Delta}(\cos\sqrt{\Delta}t - \cos 3\sqrt{\Delta}t), \tag{32}$$

since the initial conditions are

$$x_{10}(0) = 0, \quad \dot{x}_{10}(0) = 0. \tag{33}$$

For $\delta_{10} = 1$ and $A_0 C_0 D_0 = \dot{X}_0$, $A_0 S_0 = 0$, the solution of Eq. (27) yields

$$x_{10} = -\frac{\dot{X}_0}{8\Delta}(3\sin\sqrt{\Delta}t - \sin 3\sqrt{\Delta}t). \tag{34}$$

Substituting Eqs. (32) and (34) into Eq. (28) and eliminating the secular terms, we obtain

$$\delta_{11} = 0 \quad \text{for } A_0 = X_0 \text{ and } C_0 = 0 \tag{35}$$

and

$$\delta_{11} = -\frac{1}{8\Delta} \quad \text{for } A_0 = \dot{X}_0 \text{ and } S_0 = 0. \tag{36}$$

Using Eqs. (4) (17), (26), (30) and (35) or Eq. (31) and (36), the transient curves in the first approximation are obtained

$$\delta = 1 - \varepsilon + \frac{\varphi X_0^2}{2} \tag{37}$$

and

$$\delta = 1 + \varepsilon + \frac{\varphi \dot{X}_0^2}{2}\left(1 - \frac{3\varepsilon}{4\Delta}\right). \tag{38}$$

For the special case when the value of the initial deflection is equal to the initial velocity, i.e.,

$$\varepsilon_1 = 3\varphi A_0^2 = 3\varphi X_0^2 = 3\varphi \dot{X}_0^2, \tag{39}$$

the special forms of the transient curves are obtained

$$\delta = 1 + \frac{\varepsilon_1}{6} - \varepsilon \tag{40}$$

and

$$\delta = 1 + \frac{\varepsilon_1}{6} + \varepsilon\left(1 - \frac{\varepsilon_1}{8(1 - (\varepsilon_1/3))}\right). \tag{41}$$

In Fig. 2 the transient surfaces in $\varepsilon_1\delta\varepsilon$ space are plotted. The transient values depend strongly on the coefficient of nonlinearity and the initial conditions. This is a main difference in comparison to the linear systems described by the Mathieu equation [16], whose transient values are independent of the initial conditions. The dependence of the transient values on the initial conditions goes along with the general characteristic of nonlinear systems that their dynamic properties are affected by the initial conditions. For the combinations of

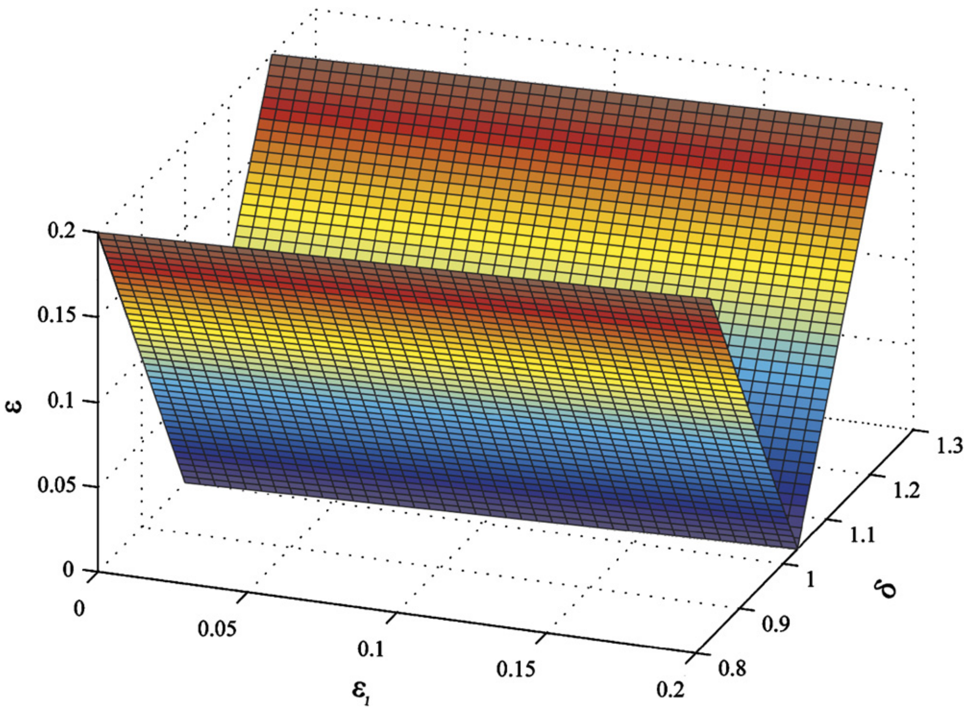


Fig. 2. The transient surfaces corresponding to the solution with the frequency $\omega_0 = 1$.

parameter $\delta$, $\varepsilon_1$ and $\varepsilon$ defined by Eqs. (40) and (41), i.e. for those lying on the surfaces, the motion is periodic with the period $4K(\sqrt{\varepsilon_1/6})$.

(3) For the period $2K(k)$ the frequency is $\omega_0 = 2$ and the solution of the differential equation $(5)_1$ is

$$x_0 = A_1 \frac{\mathrm{sn}_1 C_1 D_1 - \mathrm{cn}_1 \mathrm{dn}_1 S_1}{1 - k_1^2 \mathrm{sn}_1^2 S_1^2}, \tag{42}$$

where $\mathrm{cn}_1 \equiv \mathrm{cn}(2t, k_1)$, $\mathrm{sn}_1 \equiv \mathrm{sn}(2t, k_1)$, $\mathrm{dn}_1 \equiv \mathrm{dn}(2t, k_1)$, $S_1 = \mathrm{sn}(\alpha_1, k_1)$, $C_1 = \mathrm{cn}(\alpha_1, k_1)$, $D_1 = \mathrm{dn}(\alpha_1, k_1)$ with the modulus of the elliptic function and the parameter value

$$k_1^2 = \frac{\varphi A_1^2}{8}, \quad \delta_0^1 = 4 + \frac{\varphi A_1^2}{2}. \tag{43}$$

The initial amplitude and phase satisfy the relations

$$A_1 = \sqrt{X_0^2 + \frac{\dot{X}_0^2}{4 - (\varphi/2)X_0^2}}, \quad \mathrm{sn}\left(\alpha_1, \frac{\varphi A_1^2}{8}\right) = \frac{X_0}{A_1}. \tag{44}$$

Assuming that $k_1^2 \ll 1$ and using the transformations of the elliptic into circular function (22), Eq. $(5)_2$ is transformed into

$$\begin{aligned} &\ddot{x}_1 + 4\Delta_1 x_1 + \varepsilon_1 x_1 S_1 C_1 D_1 \sin 4\sqrt{\Delta_1} t - \frac{\varepsilon_1}{2} x_1 (S_1^2 - C_1^2 D_1^2) \cos 4\sqrt{\Delta_1} t \\ &\quad = -\delta_1 A_1 (C_1 D_1 \sin 2\sqrt{\Delta_1} t - S_1 \cos 2\sqrt{\Delta_1} t) - A_1 C_1 D_1 \sin 4\sqrt{\Delta_1} t \\ &\qquad + A_1 S_1 (1 + \cos 4\sqrt{\Delta_1} t), \end{aligned} \tag{45}$$

where

$$\Delta_1 = 1 + \frac{\varepsilon_1}{24}(1 - 3C_1^2 D_1^2 - 3S_1^2). \tag{46}$$

Using the series expansion in Eq. (26) with respect to the small parameter $\varepsilon_1$, the differential equation for $\varepsilon_1^0$ is obtained

$$\begin{aligned}\ddot{x}_{10} + 4\Delta_1 x_{10} = & -\delta_{10} A_1 (C_1 D_1 \sin 2\sqrt{\Delta_1} t - S_1 \cos 2\sqrt{\Delta_1} t) \\ & - A_1 C_1 D_1 \sin 4\sqrt{\Delta_1} t + A_1 S_1 (1 + \cos 4\sqrt{\Delta_1} t).\end{aligned} \tag{47}$$

Eliminating the secular terms in Eq. (47) it is clear that

$$\delta_{10} = 0 \tag{48}$$

and the solution is

$$x_{10} = \frac{A_1 S_1}{\Delta_1}\left(1 - \frac{14}{15}\cos 2\sqrt{\Delta_1} t - \frac{1}{15}\cos 4\sqrt{\Delta_1} t\right) - \frac{A_1 C_1 D_1}{15\Delta_1}(2\sin 2\sqrt{\Delta_1} t - \sin 4\sqrt{\Delta_1} t), \tag{49}$$

where

$$\sqrt{\Delta_1} \approx 1 + \frac{\varepsilon_1}{48}(1 - 3C_1^2 D_1^2 - 3S_1^2). \tag{50}$$

Substituting Eq. (49) into Eq. (45) and eliminating the secular terms, yields

$$\delta_{11} = -\frac{1}{24\Delta_1} \quad \text{for} \quad A_1 = \frac{\dot{X}_0}{2} \quad \text{and} \quad S_1 = 0 \tag{51}$$

and

$$\delta_{11} = \frac{1}{24\Delta_1} \quad \text{for} \quad A_1 = X_0 \quad \text{and} \quad C_1 = 0. \tag{52}$$

According to the previous considerations, the following two transient curves are obtained:

$$\delta = 4 + \frac{\varphi \dot{X}_0^2}{8} - \varepsilon \frac{\varphi \dot{X}_0^2}{32 - 2\varphi \dot{X}_0^2} \tag{53}$$

and

$$\delta = 4 + \frac{\varphi X_0^2}{2} + \varepsilon \frac{\varphi X_0^2}{8 - 2\varphi X_0^2}. \tag{54}$$

The special case when the value of the initial deflection is twice the initial velocity and

$$\varepsilon_1 = 3\varphi A_1^2 = 3\varphi X_0^2 = \frac{3}{4}\varphi \dot{X}_0^2, \tag{55}$$

gives the transient curves

$$\delta = 4 + \frac{\varepsilon_1}{6} - \frac{\varepsilon\varepsilon_1}{24 - 2\varepsilon_1} \tag{56}$$

and

$$\delta = 4 + \frac{\varepsilon_1}{6} + \frac{\varepsilon\varepsilon_1}{24 - 2\varepsilon_1}. \tag{57}$$

In Fig. 3 the transient surfaces in $\varepsilon_1\delta\varepsilon$ space are shown. The transient values depend strongly on the values of $\varepsilon_1$. It is evident that for the linear case when $\varepsilon_1 = 0$ we obtain $\delta = 4$, which is the well known critical value for a linear system.

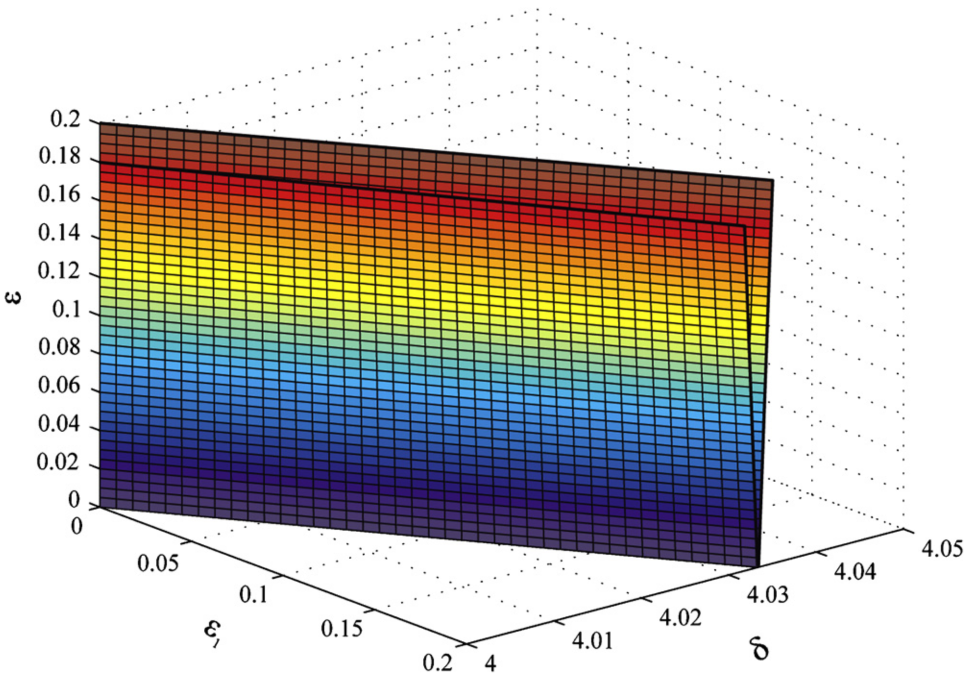


Fig. 3. The transient surfaces corresponding to the solution with the frequency $\omega_0 = 2$.

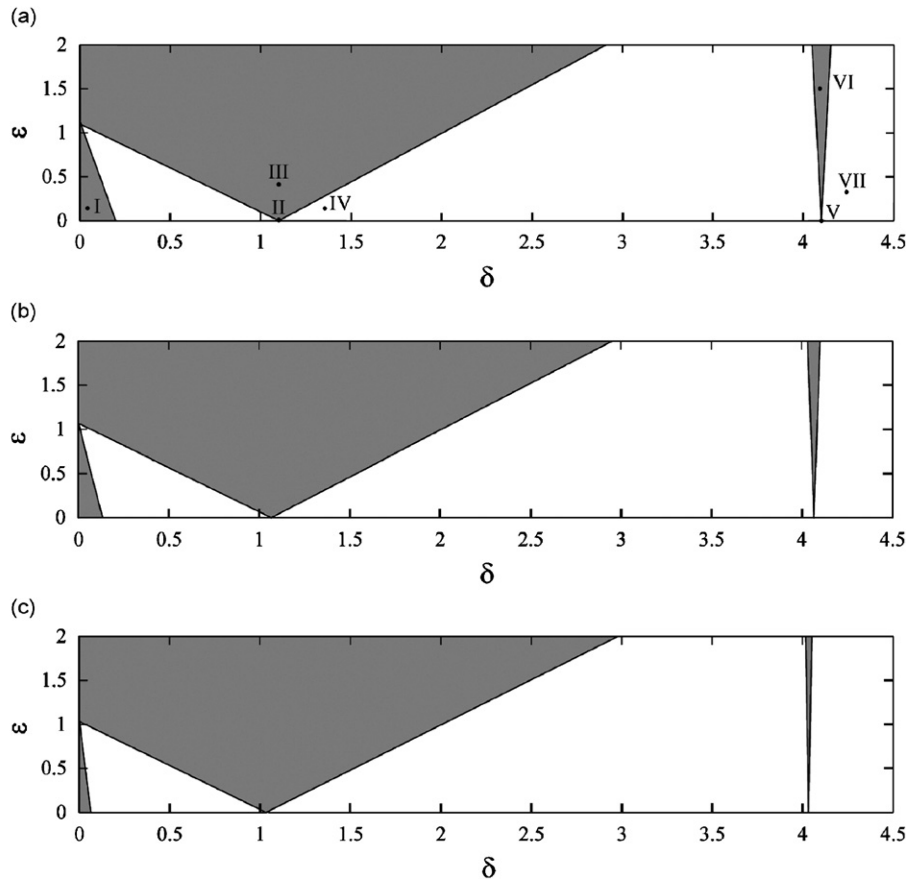


Fig. 4. Parameter $\delta\varepsilon$-plane for various values of $\varepsilon_1$: (a) $\varepsilon_1 = 0.6$, (b) $\varepsilon_1 = 0.4$, (c) $\varepsilon_1 = 0.2$.

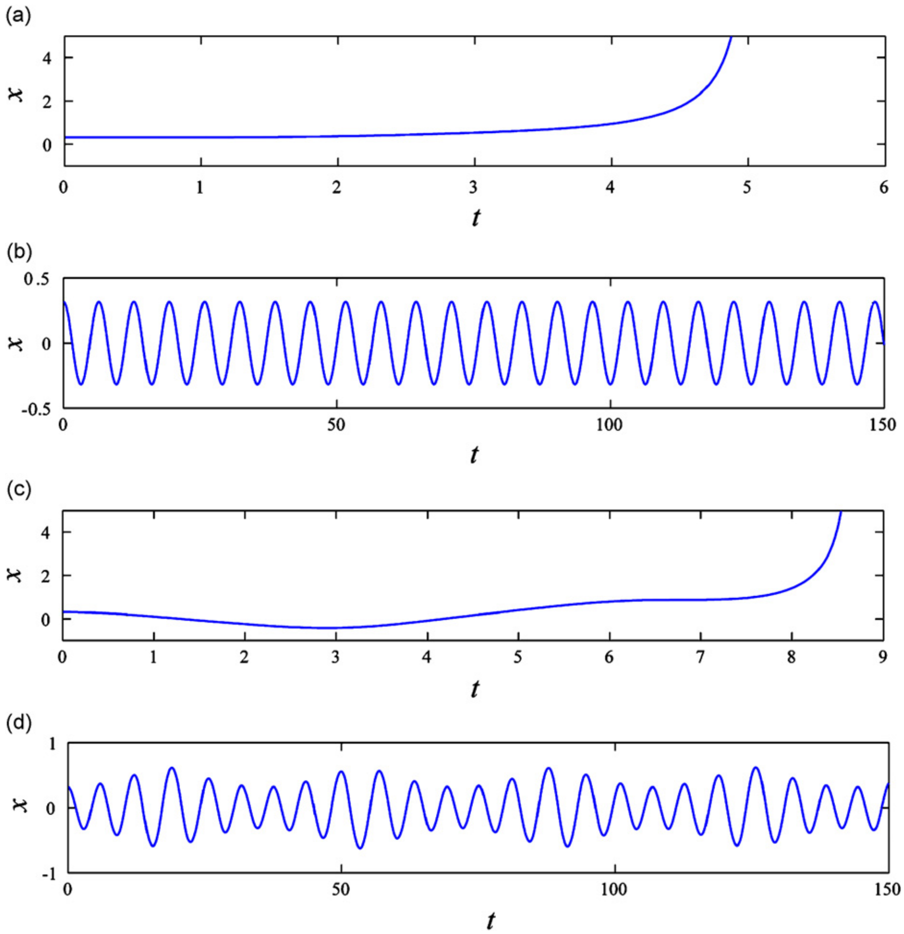


Fig. 5. The history diagrams $x$-$t$ for the points: (a) I, (b) II, (c) III, (d) IV shown in Fig. 4a.

## 3. Numerical simulation

As a demonstration and check of the validity of the approximations in this paper, the theoretical predictions are compared with the results from direct numerical integration.

Using Eqs. (15), (40), (41), (56) and (57), the parameter $\delta\varepsilon$-planes for various values of $\varepsilon_1$ are plotted in Fig. 4. For the values in the shaded regions the solution implies unbounded motion. For the values in the non-shaded regions it is bounded. The higher the values of the parameter $\varepsilon_1$, the more the shaded regions are translated to the right. This is because the parameter describing nonlinearity together with the initial conditions cause the critical values of $\delta$ to be higher than the corresponding value for the linear case [16]. Also, the regions corresponding to unbounded solutions are wider if $\varepsilon_1$ is larger. Furthermore, for small positive values of $\delta$ a region of unbounded ones exists. This is the main difference in comparison to the linear parametrically excited oscillator, for which there is a region of bounded motion in the small positive neighborhood of the origin [16].

Choosing some points from the stability chart (see Fig. 4a, points I–VII), the numerical procedure is carried out for $\varphi = 2$ and the initial conditions $x(0) = 0.3162$, $\dot{x}(0) = 0$ (Figs. 5 and 6). The parameters corresponding to these points are: point I: $\varepsilon = 0.1$, $\delta = 0.08$; point II: $\varepsilon = 0$, $\delta = 1.1$; point III: $\varepsilon = 0.4$, $\delta = 1.1$; point IV: $\varepsilon = 0.1$, $\delta = 1.25$ (Fig. 5); point V: $\varepsilon = 0$, $\delta = 4.1$; point VI: $\varepsilon = 1.5$, $\delta = 4.1$; point VII: $\varepsilon = 0.3$, $\delta = 4.2$ (Fig. 6). While Fig. 5 shows the time history diagrams, in Fig. 6 both time history diagrams and the corresponding phase planes are plotted. The numerical results convey the results of the analytical analysis.

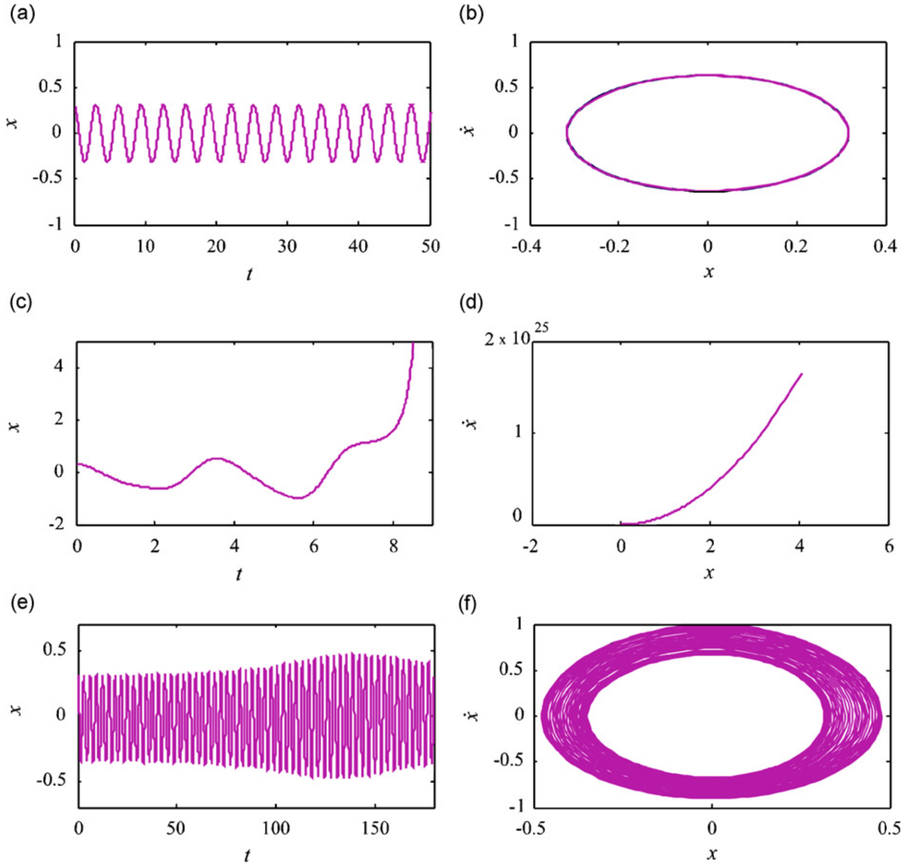


Fig. 6. The history diagrams $x$–$t$ and phase curves $x$–$\dot{x}$ for $\varphi = 2$, $x(0) = 0.3162$, $\dot{x}(0) = 0$ for the points V–VII shown in Fig. 4a: (a), (b) V: $\varepsilon = 0$, $\delta = 4.1$; (c), (d) VI: $\varepsilon = 1.5$, $\delta = 4.1$; (e), (f) VII: $\varepsilon = 0.3$, $\delta = 4.2$.

## 4. Conclusion

A first-order analytical solution of the Mathieu–Duffing differential equation has been obtained by using the two dimensional Linstedt–Poincare perturbation method. The unperturbed equation includes strong negative cubic nonlinearity, whose exact solution is given with Jacobi elliptic functions. The transition curves along which the periodic solutions with period $2K$ and $4K$ exist, have been constructed. Based on the obtained results, the following can be concluded:

1. The analytical results show that the nonlinearity significantly changes the characteristics of parametric resonance and the presence of a negative cubic nonlinearity alters the dynamic behavior of the system.

2. The use of the elliptic functions instead of the trigonometric functions has a principle advantage since the subharmonic resonances of all orders are accounted for.

3. The transient values are dependent on the initial conditions. In the special case when the value of $\varphi$ is chosen to be zero, the transient curves are equivalent to those corresponding to the linear Mathieu equation. It has been shown that any small deviations from those transition curves leads to the complete loss of periodicity.

4. Comparing the approximate analytical and numerical results it is shown that the results obtained for the small values of $\varepsilon$ agree well during the initial time period.


## Acknowledgment

This investigation is supported by the Ministry of Science and Environmental Protection, Republic of Serbia (Project No. 144008).

## References

[1] M. Mond, G. Cederbaum, Stability analysis of the non-linear Mathieu equation, *Journal of Sound and Vibration* 167 (1) (1993) 77–89.
[2] E. Esmailzadeh, G.N. Jazar, B. Mehri, Existence of periodic solution for beams with harmonically variable length, *ASME Journal of Vibration and Acoustics* 119 (3) (1997) 485–488.
[3] E. Esmailzadeh, N. Jalili, Parametric response of cantilever Timoshenko beams with tip mass under harmonic support motion, *International Journal of Non-Linear Mechanics* 33 (5) (1998) 765–781.
[4] E. Esmailzadeh, A. Goodarzi, Stability analysis of a CALM floating offshore structure, *International Journal of Non-Linear Mechanics* 36 (6) (2001) 917–926.
[5] Y.O. El-Dib, Nonlinear Mathieu equation and coupled resonance mechanism, *Chaos Solitons and Fractals* 12 (4) (2001) 705–720.
[6] L. Ng, R. Rand, Bifurcations in a Mathieu equation with cubic nonlinearities, *Chaos, Solitons and Fractals* 14 (2002) 173–181.
[7] L. Ng, R. Rand, Bifurcations in a Mathieu equation with cubic nonlinearities, *Communications in Nonlinear Science and Numerical Simulation* 7 (Part II) (2002) 107–121.
[8] J.F. Rhoads, S.W. Shaw, K.L. Turner, J. Moehlis, B.E. DeMartini, W. Zhang, Generalized parametric resonance in electrostatically actuated microelectromechanical oscillators, *Journal of Sound and Vibration* 296 (2006) 797–829.
[9] V.N. Belovodsky, S.L. Tsyfansky, V.I. Beresnevich, The dynamics of a vibromachine with parametric excitation, *Journal of Sound and Vibration* 254 (5) (2002) 897–910.
[10] G.T. Abraham, A. Chatterjee, Approximate asymptotic solution for nonlinear Mathieu equation using harmonic balance based averaging, *Nonlinear Dynamics* 31 (2003) 347–365.
[11] M. Wiegand, S. Scheithauer, S. Theil, Step proof mass dynamics, *Acta Astronautica* 54 (2004) 631–638.
[12] W. Zhang, R. Baskaran, K.L. Turner, Effect of cubic nonlinearity on auto-parametrically amplified resonant MEMS mass sensor, *Sensors and Actuators A* 102 (2002) 139–150.
[13] D. Younesian, E. Esmailzadeh, R. Sedaghati, Existence of periodic solutions for the generalized form of Mathieu Equation, *Nonlinear Dynamics* 39 (2005) 335–348.
[14] L. Cveticanin, Vibrations in a parametrically excited system, *Journal of Sound and Vibration* 229 (2) (2000) 245–271.
[15] G.N. Jazar, Stability chart of parametric vibrating systems using energy-rate method, *International Journal of Non-Linear Mechanics* 39 (2004) 1319–1331.
[16] A.H. Nayfeh, D.T. Mook, *Nonlinear Oscillations*, Wiley, New York, 1979.
[17] J. Li, W. Xu, Z. Ren, Y. Lei, Maximal Lyapunov exponent and almost-sure stability for stochastic Mathieu–Duffing systems, *Journal of Sound and Vibration* 286 (2005) 395–402.
[18] R.S. Zounes, R.H. Rand, Subharmonic resonance in the non-linear Mathieu equation, *International Journal of Non-Linear Mechanics* 37 (2002) 43–73.
[19] P.F. Byrd, M.D. Friedman, *Handbook of Elliptic Integrals for Engineers and Physicists*, Springer, Berlin, 1954.
[20] M. Abramowitz, I.A. Stegun, *Handbook of Mathematical Functions with Formulas, Graphs and Mathematical Tables*, Nauka, Moscow, 1979.